

Secular Instability and Planetesimal Formation in the Dust Layer

J. GOODMAN

B. PINDOR

Princeton University Observatory, Princeton, NJ 08544

Email: `jeremy@astro.princeton.edu`

ABSTRACT

Late in the gaseous phase of a protostellar disk, centimeter-sized bodies probably settle into a thin “dust layer” at the midplane. A velocity difference between the dust layer and the gas gives rise to turbulence, which prevents further settling and direct gravitational instability of the layer. The associated drag on the surface of the layer causes orbital decay in a few thousand years—as opposed to a few hundred years for an isolated meter-sized body. Within this widely-accepted theoretical framework, we show that the turbulent drag causes radial instabilities even if the selfgravity of the layer is negligible. We formulate axisymmetric, height-integrated dynamical equations for the layer that incorporate turbulent diffusion of mass and momentum in radius and height, vertical settling, selfgravity, and resistance to compression due to gas entrained within the dust layer. In steady-state, the equations describe the inward radial drift of a uniform dust layer. In perturbation, overdense rings form on an orbital timescale with widths comparable to the dust-layer thickness. Selfgravity is almost irrelevant to the linear growth rate but will eventually fragment and collapse the rings into planetesimals larger than a kilometer. We estimate that the drag instability is most efficient at 1 AU when most of the “dust” mass lies in the size range 0.1-10 meters.

Subject headings: planetesimals; planetary formation

1. INTRODUCTION

Meteoritic evidence and theoretical considerations indicate that planet formation begins with collisional agglomeration of dust particles into larger bodies during the lifetime of a gaseous protostellar disk ($\lesssim 10^7$ yr).

Because the gas is partly supported against the gravity of the central star by pressure, the orbital velocity of the disk is slightly lower than the keplerian circular velocity ($V_K = \sqrt{GM/r}$). If c_s is the sound speed of the gas, then

$$\eta \equiv \frac{V_K - V_{\text{gas}}}{V_K} \approx -\frac{r}{2\rho_g V_K^2} \frac{\partial P}{\partial r} \sim \left(\frac{c}{V_K}\right)^2. \quad (1)$$

Solid bodies couple to the gas by aerodynamic drag and orbit at intermediate velocities. Small grains move almost exactly with the gas, while large planetesimals move nearly at V_K . In both limits, drag causes very little dissipation of orbital energy. Dissipation is maximal for bodies of intermediate size. At 1 AU in a minimum-mass solar nebula (Hayashi et al. 1985), the orbital decay time is only a few hundred years for particle radii $r_p \sim 1$ m (cf. §2). Therefore, the processes responsible for growth must move bodies rapidly through the intermediate size range. Since the orbital decay time scales roughly linearly with r_p above ~ 1 m, planetesimals larger than $r_p \sim 10$ km experience little decay during the lifetime of the nebula.

While collisional agglomeration may be sufficient to reach \gtrsim km size before the orbits decay, collective instability is an attractive alternative. Safronov (1969) and Goldreich & Ward (1973, henceforth GW) suggested that planetesimals may form by gravitational instability. As an initially turbulent disk becomes quiescent, or as the solid bodies grow to radii $r_p \sim 1$ cm, the particles settle into an increasingly dense layer—the “dust layer”—at the midplane. When the volume-averaged density of the dust layer approaches $\rho_* \equiv 3M/4\pi a^3$, where M is the mass of the star and a is the orbital radius, the layer becomes gravitationally unstable. Self-gravity then fragments the layer into planetesimals with radii ~ 1 km.

Gravitational instability along the above lines is now regarded as unlikely. The dust layer would have to be very much thinner than the gas disk, since the mass fraction of solids at solar abundances is small ($\sim 10^{-2}$), and since the gas density itself is already $\sim 10^{-2}\rho_*$ in a minimum-mass solar nebula. On the other hand, the velocity shear between the dust layer and the gas probably causes turbulence, even if there is no other source of turbulence in the gas disk. Although GW called attention to this “boundary-layer” turbulence, they considered its implications only for the exchange of momentum between the dust layer and the gas. Weidenschilling (1980) pointed out that turbulence will also tend to limit the density of the dust layer by mixing. More recently, Cuzzi et al. (1993, henceforth CDC) have confirmed this with a detailed analysis particle settling, shear-driven turbulence, and turbulent vertical mixing. These authors conclude that gravitational instability is unlikely to occur at 1 AU until $r_p \gg 1$ m, if at all.

Even if direct gravitational instability does not occur, there may be secular instabilities—that is, instabilities relying upon dissipation. GW mentioned the possibility of secular effects but did not elaborate. They may have had in mind the following axisymmetric instability: Consider a steady background state in which the surface mass density of the dust layer (Σ_p) is uniform on scales $\ll r$ and drifts radially inward at a rate proportional to the drag against the gas. Let there be a positive perturbation in Σ_p on a ring of radial width (Δr) smaller than the thickness of the gas layer (H_g) but larger than that of the dust layer (H_p). The (slight) selfgravity of the ring reinforces the gravitational attraction of the star on the dust layer at the outer edge of the ring, and has the opposite effect at the inner edge of the ring. These gravitational perturbations must be balanced by pressure gradients or centrifugal forces. Since $H_p < \Delta r < H_g$, the orbital speed of the gas is much less affected than the orbital speed of the dust, which increases at the outer edge of the ring and decreases at the inner edge. The outer (inner) edge suffers greater (less) drag

and a larger (smaller) inward radial drift rate. This reinforces the perturbation in Σ_p . Drag is clearly essential: without it, contraction of the dense ring would be prevented for $\Delta r \gg H_p$ by the difference in specific angular momentum between the inner and outer edges of the ring; but drag changes the angular momentum of the dust. The planform of the secular instability is expected to be stationary in a frame drifting inward with the dust layer. Safronov (1991) remarked that the layer will probably be stabilized by the difference in radial drift speed among bodies of different size. This assumes that the drag acts separately on individual bodies. Many theoretical studies of the dust layer (including GW and CDC), however, assume that the drag acts collectively because the gas *within* the layer is entrained by the greater mass of solids. In §4, we shall find that whether the particles feel the drag individually or collectively depends upon their size. For the present, we take the drag to be collective.

The original intent of the present work was to study the secular gravitational instability described above. We expected to find a slowly growing mode (compared to the orbital frequency) on scales $\Delta r \gg H_p$, whose growth rate would tend to zero with ρ/ρ_* . But our analysis uncovered a rapid, small-scale, drag-driven instability that does not require any selfgravity, although it does require that the drag be collective.

The structure of this paper is as follows. In §2, we present height-integrated nonlinear equations for the axisymmetric evolution of the dust layer based largely upon the work of CDC, and we cast these equations into dimensionless form. We also discuss our assumptions for the nebular parameters, and we find steady solutions to the equations in which the surface density is locally uniform. The linear stability of the steady solutions is examined in §3, first analytically and then semi-numerically. The most rapid instabilities are driven by drag rather than selfgravity. The following section, §4, explores a number of important issues, including the collective nature of the drag force, the relative importance of the instability for building planetesimals compared to straightforward collisional agglomeration, and the expected planetesimal mass if the instability dominates. §4 also briefly compares this work with some notable previous investigations of the stability of protoplanetary disks that treat gas and dust as dynamically distinct components (Coradini et al. 1981; Sekiya & Nakagawa 1988; Noh et al. 1991). §5 sums up.

2. PHYSICAL MODEL AND GOVERNING EQUATIONS

The purpose of this section is to develop model equations for axisymmetric radial perturbations of the dust layer. To avoid having to treat two spatial dimensions at once, we adopt a height-integrated approximation based upon the results of CDC, whose notation we generally follow. Important physical influences on the evolution of the dust layer include turbulent drag against the gas; turbulent mixing, horizontally as well as vertically; gas pressure (which resists compression of the layer); and selfgravity.

We are concerned with a late phase in the evolution of the gaseous protoplanetary nebula when

accretion and its attendant turbulence have subsided, allowing the dust to settle into a thin layer of half-thickness H_p very much less than that of the gas, H_g (Safronov 1969; Goldreich & Ward 1973). (In this paper, “dust” refers indiscriminantly to all solids smaller than a few meters.) Within the dust layer, the volume-averaged mass density of the dust (ρ_p) exceeds that of the gas (ρ_g), as shown below, but the column density of the gas ($\Sigma_g \approx 2H_g\rho_g$) greatly exceeds that of the dust ($\Sigma_p \approx 2H_p\rho_p$). At solar abundance, $\Sigma_g/\Sigma_p \approx 200$ if the dust contains all materials condensible at temperatures ~ 300 K.

We assume a standard minimum-mass solar nebula with the following radial scalings:

$$\begin{aligned} T(r) &= 280 \text{ K} \left(\frac{r}{\text{AU}}\right)^{-0.5} \\ \Sigma_g(r) &= 1700 \text{ g cm}^{-2} \left(\frac{r}{\text{AU}}\right)^{-1.5} \\ \rho_g(r) &= 1.7 \times 10^{-9} \text{ g cm}^{-3} \left(\frac{r}{\text{AU}}\right)^{-2.75}. \end{aligned} \quad (2)$$

For ease of reference, we summarize the more important physical parameters in Table I.

*Table
I
here*

2.1. Turbulent drag on the dust layer

In steady state, the dust layer orbits nearly at the the keplerian velocity $V_K = \sqrt{GM/r}$, where M is the mass of the protostar, and r is the orbital radius. (Unless otherwise stated, $M = 1 M_\odot$ and $r = 1\text{AU}$.) Because of its radial pressure gradients, the gas orbits at the slightly lower velocity $(1 - \eta)V_K$ determined by equation (1). For nominal parameters, $\eta \approx 10^{-3}$ [Table I].

Because of the orbital velocity difference above, GW argued that the interface between the dust layer and the relatively pristine gas should be turbulent, even if the nebula is otherwise quiescent, by analogy with the standard laboratory situation of a thin solid plate placed edgewise in a nearly inviscid, incompressible flow. The drag on such a plate due to turbulent momentum transport is

$$\vec{F}_{\text{drag}} = -\frac{\rho_g |\Delta \vec{v}|}{\text{Re}_*} \Delta \vec{v}, \quad (3)$$

where Δv is the velocity difference between the plate and the undisturbed flow, and the “Reynolds number” Re_* is an empirical dimensionless constant. The drag law is usually stated in scalar form, $F_{\text{drag}} = -\rho_g(\Delta v)^2/\text{Re}_*$; the vectorial form above assumes that the force is antiparallel to the relative velocity. Citing laboratory measurements, GW took $\text{Re}_* \approx 500$, but CDC advocated $\text{Re}_* \approx 45 - 180$. We take $\text{Re}_* = 180$ as a reference value but are careful to note how things scale with this number.

The turbulent transfer of momentum from the dust layer (or flat plate) to the surrounding medium is effectively diffusive and can be described by a *turbulent viscosity* ν_T , with dimensions of $(\text{length})^2(\text{time})^{-1}$. In order to reproduce the drag (3), one needs $\nu_T \approx L\Delta v/\text{Re}_*$, where L is the vertical thickness of the *turbulent boundary layer*—the layer within which the velocity, though

fluctuating, is closer to that of the dust layer than to that of the undisturbed gas. As noted by GW, L should be comparable to the Ekman length constructed upon ν_T and the orbital angular velocity Ω :

$$L_E = \left(\frac{\nu_T}{\Omega}\right)^{1/2}. \quad (4)$$

Viewed in inertial coordinates, the direction of the stress exerted by the dust layer on the gas rotates during the orbit, and L_E is the vertical distance over which horizontal momentum diffuses in time Ω^{-1} . Similar considerations govern the thickness of the boundary layer at the base of the Earth’s atmosphere (Pedlosky 1987). As a generic measure of the boundary-layer thickness, CDC take $L = c_L L_E$ with $c_L = 1.5$. Since $\nu_T \approx L\Delta v/\text{Re}_*$, it follows that

$$\nu_T \approx \frac{c_L^2 \Delta v^2}{\Omega \text{Re}_*^2}, \quad (5)$$

and also that

$$L \approx \frac{c_L \Delta v}{\text{Re}_* \Omega}. \quad (6)$$

The factors involving Re_* in eqs. (3), (5), and (6) represent significant corrections to naive dimensional analysis. They are semi-empirical, based upon terrestrial experience that may not be a reliable guide to the situation we wish to study. However, it seems difficult to improve upon these factors without resort to an ambitious three-dimensional hydrodynamic simulation.

2.2. Thickness of the dust layer

The equilibrium half-thickness $H_{p,0}$ of the dust layer results from competition between turbulent stirring and gravitational settling. Following CDC, we assume that H_p is comparable to the *1% boundary-layer thickness*—the height above the midplane at which the mean azimuthal velocity is within 1% of its asymptotic value far above the dust. Also following CDC, we take this thickness to be larger than L by a factor $c_\delta \approx 2.5$. Thus,

$$H_{p,0} = c_\delta c_L \frac{\Delta v}{\Omega \text{Re}_*}. \quad (7)$$

Unless otherwise noted, we adopt eq. (7) for the dust-layer thickness. We believe that it is appropriate for dust-particle sizes of order 10 cm. But the layer is likely to be somewhat thicker (thinner) if the particles are much smaller (larger) than this.

When all particles are small they will be tightly coupled to the gas within the dust layer by drag (see below). In this limit, where the settling time is effectively infinite and the slightest turbulence is sufficient to loft the dust, the equilibrium vertical distribution of dust is likely to occur at the point of marginal shear instability, absent other sources of turbulence. The following is a simplified estimate of the thickness under these assumptions; a more careful treatment has been given by

Sekiya (1999). Shear instability is expected only if the Richardson number

$$Ri \equiv \frac{(\partial\Phi/\partial z)(\partial \ln \rho/\partial z)}{(\partial v/\partial z)^2} \leq \frac{1}{4}. \quad (8)$$

The vertical gravitational potential $\Phi(z)$ is $\Omega^2 z^2/2$, and the horizontal velocity $v(z)$ (relative to the keplerian value V_K) is determined by the geostrophic balance

$$2\rho\Omega v = \frac{\partial P}{\partial r}. \quad (9)$$

For simplicity, we take gaussian profiles for both the dust and the gas, $\rho_p(z) = \rho_p(0)e^{-z^2/2H_p^2}$ and $\rho_g(z) = \rho_g(0)e^{-z^2/2H_g^2}$, with $H_p \ll H_g$. Then since $v(z) \rightarrow -\eta V_K$ when $z \gg H_p$,

$$\begin{aligned} \rho(z) &= \rho_g(z) + \rho_p(z) \approx \rho(0) \left(1 - f + f e^{-z^2/2H_p^2}\right) \\ v(z) &\approx -\eta V_K \left(1 + \frac{f}{1-f} e^{-z^2/2H_p^2}\right)^{-1}, \end{aligned}$$

where $f \equiv \rho_p(0)/\rho(0)$ is the fractional contribution of the dust to the total density at the midplane. With these assumptions, $Ri(z) \approx Ri(0)$ within one scale height of the midplane, and increases at higher altitudes.

$$Ri(0) = \left(\frac{\Omega H_p}{\eta V_K}\right)^2 \frac{(1-f)^2}{f^3}$$

On the other hand,

$$\frac{\rho_p(0)H_p}{\rho_g(0)H_g} = \frac{\Sigma_p}{\Sigma_g} \equiv Z_p,$$

where $Z_p \approx 0.005$ is the fractional abundance of dust. Together with $H_g = c_s/\Omega \approx \eta^{1/2}V_K$, these relations imply that the condition $Ri(0) \leq 1/4$ is equivalent to

$$\frac{\rho_p(0)}{\rho(0)} \geq \left(\frac{4Z_p^2}{\eta}\right)^{1/3} \approx 0.46,$$

i.e. about equal contributions to the midplane density from dust and gas. It follows that the dust-layer thickness in the limit of very small particles is

$$(H_p)' = \frac{1-f}{f} Z_p H_g \lesssim 0.18 \frac{\eta V_K}{\Omega} \quad (10)$$

This is about 9 times larger than our standard estimate (7) if we take $Re_* = 180$ and $\Delta v = \eta V_K$. In the small-particle limit where (10) holds, there may be very little drag on the dust layer, since the turbulence is only incipient.

Larger particles are imperfectly coupled to the gas, and significant turbulence will be required to keep them from settling. A dimensionless measure of the strength of drag coupling is Ωt_s , where the “stopping time” t_s is the decay time of the velocity of an isolated particle relative to the gas

if subject to no forces other than drag. As discussed by CDC and others, there are at least three distinct drag regimes of interest, distinguished by the relative sizes of the the particle radius (r_p), the molecular mean-free path (λ), the sound speed (c), and the relative velocity between particle and gas (v_{rel}). Particles with radii $r_p \leq 9\lambda/4$ are in the “Epstein” regime, where the velocities of gas molecules striking the particle are uncorrelated with that of the particle itself, and the drag force is $4\pi r_p^2 \rho_g c v_{\text{rel}}/3$. If $r_p > 9\lambda/4$ but $r_p < \lambda c/(4v_{\text{rel}})$, there is a laminar viscous flow over the particle, and the drag is given by Stokes’ formula $6\pi\mu r_p v_{\text{rel}}$, where $\mu \approx \rho_g \lambda c/2$ is the dynamical viscosity of the gas. At still larger values of r_p and/or v_{rel} , the flow over the particle is turbulent and the drag force increases faster than linearly with v_{rel} , eventually quadratically. The mean-free path $\lambda \approx 1(r/\text{AU})^{2.75} \text{cm}$ at the midplane of the nebula (2). Thus

$$t_s \approx \begin{cases} 1.2 \times 10^4 (r_p/\text{cm})(r/\text{AU})^3 \text{ s} & \text{“Epstein”}, \\ 5.3 \times 10^3 (r_p/\text{cm})^2 (r/\text{AU})^{2.75} \text{ s} & \text{“Stokes”}, \end{cases} \quad (11)$$

with the dividing line between the two regimes at $r_p \approx 2.3(r/\text{AU})^{2.75} \text{cm}$. Presuming that $v_{\text{rel}} < \eta\Delta v$, the turbulent regime requires $r_p > 10(r/\text{AU})^{2.5} \text{cm}$.

Since the vertical gravitational acceleration is $\Omega^2 z$, a particle settling through quiescent gas reaches a terminal velocity $\Omega^2 z/t_s$ provided $\Omega t_s < 1$, so that z decays exponentially at the rate

$$\gamma_s^{-1} \equiv (\Omega^2 t_s)^{-1}. \quad (12)$$

Turbulence will resist this settling. Following CDC, we describe turbulent stirring by a mass-diffusion coefficient

$$\nu_{\text{mass}} = \frac{\nu_T}{\text{Sc}}. \quad (13)$$

where the “Schmidt number” $\text{Sc} \geq 1$ describes the efficiency with which turbulent eddies are able to pick up the particles; Sc increases with particle size and with orbital radius in the nebula [cf. Fig. 2 in CDC]. Therefore, still another estimate of the dust-layer thickness, H_p'' , follows from equating the diffusion rate ν_{mass}/H_p^2 to the settling rate $\Omega^2 t_s$:

$$H_p'' = \left(\frac{\nu_T}{\text{Sc}\Omega^2 t_s} \right)^{1/2} = \frac{H_p}{c_\delta \sqrt{\text{Sc}\Omega t_s}}. \quad (14)$$

For 10-cm particles at 1 AU, $\text{Sc} \approx 3$ and the thicknesses (7) and (14) are comparable. For much smaller particles, where $H_p'' > H_p$, the turbulence and its associated drag are probably incompletely developed, so that the estimate (10) is probably more accurate. For larger particles or larger orbital radii, H_p'' is smaller than H_p , so that in using eq. (7) for the thickness, we are probably underestimating the effects of selfgravity.

2.3. Vertically integrated equations of motion

Here we lay out the equations of motion for the dust layer in a height-averaged approximation. The gas above and below the dust layer is taken to be undisturbed, on the grounds that we are

concerned with radial scales Δr that are somewhat greater than H_p but $\ll H_g$. Disturbances in the pressure and density of overlying gas are expected to equilibrate on a timescale

$$\frac{\Delta r}{c} \approx \frac{\Delta r}{H_g} \Omega^{-1} \ll \Omega^{-1},$$

whereas we shall be concerned with motions of the dust layer over times $\gtrsim \Omega^{-1}$. We shall allow, however, for the pressure of the gas trapped within the dust layer.

We write U and $V + V_K$ for the vertically-averaged radial and azimuthal velocities of the dust layer:

$$\begin{aligned} \Sigma_p(r, t) &= \int_{-\infty}^{\infty} \rho_p(r, t, z) dz, \\ \begin{Bmatrix} U(r, t) \\ V(r, t) \end{Bmatrix} &= \frac{1}{\Sigma_p(r, t)} \int_{-\infty}^{\infty} \rho_p(r, t, z) \begin{Bmatrix} v_r(r, t, z) \\ v_\phi(r, t, z) - V_K(r) \end{Bmatrix} dz. \end{aligned}$$

Continuity of dust mass is expressed by

$$\frac{\partial \Sigma_p}{\partial t} + \frac{1}{r} \frac{\partial}{\partial r} \left[r \left(U \Sigma_p - \nu \frac{\partial \Sigma_p}{\partial r} \right) \right] = 0.$$

The term involving ν reflects our assumption that if the turbulence mixes the particles vertically, then it also mixes them radially. For want of a better hypothesis, we take $\nu = \nu_{\text{mass}}$ [eq. (13)]. On lengthscales $\Delta r \ll r$, the metric factors r^{-1} and r surrounding the radial derivative above can be neglected, so our mass equation becomes

$$\frac{\partial \Sigma_p}{\partial t} + \frac{\partial}{\partial r} \left(U \Sigma_p - \nu \frac{\partial \Sigma_p}{\partial r} \right) = 0. \quad (15)$$

Next, we develop equations for the velocity components V and U . In axisymmetry the only azimuthal force is drag, so that if radial diffusion is neglected for the moment, then the specific angular momentum of the dust evolves as

$$\left(\frac{\partial}{\partial t} + U \frac{\partial}{\partial r} \right) [r(V + V_K)] = -r \frac{\rho_g \Delta v}{\Sigma_p \text{Re}_*} (V + \eta V_K),$$

or equivalently, since $V/r \ll \Omega$,

$$\left(\frac{\partial}{\partial t} + U \frac{\partial}{\partial r} \right) V = -\frac{\Omega U}{2} - \frac{\rho_g \Delta v}{\Sigma_p \text{Re}_*} (V + \eta V_K), \quad (16)$$

where

$$\Delta v \equiv |\Delta \vec{v}| = \sqrt{U^2 + (V + \eta V_K)^2}. \quad (17)$$

The dynamical equation for U incorporates coriolis force (the residual of centrifugal and central forces), drag, self-gravity, and pressure:

$$\left(\frac{\partial}{\partial t} + U \frac{\partial}{\partial r}\right) U = 2\Omega V - \frac{\rho_g |\Delta v|}{\Sigma_p \text{Re}_*} U - \frac{\partial \psi}{\partial r} - \frac{1}{\Sigma_p} \frac{\partial \Pi}{\partial r}. \quad (18)$$

An adequate local approximation for the acceleration due to self-gravity is

$$-\frac{\partial \psi}{\partial r}(r) \approx 2G \int_{-\infty}^{\infty} \frac{\Sigma_p(r + \Delta r) \Delta r}{(\Delta r)^2 + (H_{p,0})^2} d(\Delta r), \quad (19)$$

which is equivalent to its radial fourier transform,

$$\tilde{\psi}(k) = \int_{-\infty}^{\infty} \psi(r + \Delta r) e^{-ik\Delta r} d(\Delta r) = -\frac{2\pi G}{|k|} e^{-|k|H_{p,0}} \tilde{\Sigma}(k), \quad (20)$$

if the main contribution comes from $|\Delta r| \ll r$. The terms involving $H_{p,0}$ soften the force on scales smaller than the equilibrium dust-layer thickness. Perhaps one ought to use the actual local thickness $H_p(r, t)$ rather than its equilibrium value, but then the force could not be calculated so easily by fourier transforms. It seems pointless to accept this complication since the exact force softening depends upon the detailed shape of the vertical density profile, which is beyond the scope of the height-integrated treatment.

The height-integrated pressure involves the weight of the overlying dust:

$$\Pi(r, t) = \int_{-\infty}^{\infty} dz \int_z^{\infty} dz' \rho_p(r, t, z') \Omega^2 z' = \Sigma_p H_p^2 \Omega^2, \quad (21)$$

neglecting a factor of order unity that also depends upon the vertical density profile. This formula presupposes vertical hydrostatic equilibrium, which is justified by the thinness of the dust layer and the slowness of its motions. Only the dust density contributes to the excess pressure since the gas is neutrally buoyant.

We assume that the gas *within* the dust layer is trapped there on timescales shorter than the settling time (12). The internal (thermal) energy of this gas is large compared to the kinetic energy in the radial motions of interest, even if the trapped gas is a minor contributor to the volume mass density. On short timescales, therefore, the dust layer is three-dimensionally incompressible:

$$\frac{\delta \Sigma_p}{\Sigma_p} \approx \frac{\delta H_p}{H_p} \quad \text{and} \quad \frac{\delta \Pi}{\Pi} \approx 3 \frac{\delta \Sigma_p}{\Sigma_p}. \quad (22)$$

But H_p should relax towards equilibrium on the settling time γ_s^{-1} [eq. (12)], restoring Π to its equilibrium value. These considerations suggest the following dynamical equation for Π :

$$\left(\frac{\partial}{\partial t} + U \frac{\partial}{\partial r}\right) \Pi = -3\Pi \frac{\partial U}{\partial r} - 2\gamma_s(\Pi - \Pi_0), \quad (23)$$

where Π_0 is the equilibrium pressure.

For the purpose of nonlinear simulations, it is useful to re-cast the dynamical equations (16), (18), and (22) in “conservative” form. Multiplying eq. (16) by Σ_p and eq. (15) by V and adding the results, we have

$$\frac{\partial(\Sigma_p V)}{\partial t} + \frac{\partial(U\Sigma_p V)}{\partial r} - V\nu\frac{\partial^2\Sigma_p}{\partial r^2} = -\frac{\Omega\Sigma_p U}{2} - \frac{\rho_g\Delta v}{\text{Re}_*}(V + \eta V_K).$$

The form of the term involving ν results from our assumption that mass diffuses radially but velocities (momentum per unit mass) do not. This is unreasonable, since one already assumes that *vertical* momentum diffusion is driven primarily by vertical shear. It is very unclear, however, exactly what combination of radial derivatives of V and Σ_p to use above. There is a controversy whether hydrodynamic turbulence in a differentially rotating disk attempts to equalize angular velocity, $(V_K + V)/r$, or specific angular momentum, $r(V_K + V)$ (Balbus & Hawley 1998). Without taking a stand on this issue, we replace the diffusive term above with

$$-\nu\frac{\partial(\Sigma_p V)}{\partial r}$$

for the form of the diffusive term, and corresponding forms for the other dynamical variables. This leads to somewhat simpler equations than other plausible choices. More importantly, the radial diffusion is then unambiguously stabilizing at short wavelengths; this is a nontrivial result, because some other plausible forms of the effective viscosity actually *cause* axisymmetric instability (Schmit & Tscharnuter 1995).

Our final set of dynamical equations is therefore

$$\begin{aligned} \frac{\partial(\Sigma_p V)}{\partial t} + \frac{\partial}{\partial r} \left(U\Sigma_p V - \nu\frac{\partial(\Sigma_p V)}{\partial r} \right) \\ = -\frac{\Omega\Sigma_p U}{2} - \frac{\rho_g\Delta v}{\text{Re}_*}(V + \eta V_K), \end{aligned} \quad (24)$$

$$\begin{aligned} \frac{\partial(\Sigma_p U)}{\partial t} + \frac{\partial}{\partial r} \left(\Sigma_p U^2 - \nu\frac{\partial(\Sigma_p U)}{\partial r} \right) \\ = 2\Omega\Sigma_p V - \frac{\rho_g|\Delta v|}{\text{Re}_*}U - \Sigma_p\frac{\partial\psi}{\partial r} - \frac{\partial\Pi}{\partial r}, \end{aligned} \quad (25)$$

$$\frac{\partial\Sigma_p}{\partial t} + \frac{\partial}{\partial r} \left(U\Sigma_p - \nu\frac{\partial\Sigma_p}{\partial r} \right) = 0, \quad (26)$$

$$\frac{\partial\Pi}{\partial t} + \frac{\partial}{\partial r} \left(U\Pi - \nu\frac{\partial\Pi}{\partial r} \right) = -2\Pi\frac{\partial U}{\partial r} - 2\gamma_s(\Pi - \Pi_0), \quad (27)$$

which must be supplemented by Poisson’s equation (20).

2.4. Dimensionless units

It is convenient to adopt the system of units and dimensionless variables described in Table II, in which r_0 is a radius characteristic of the region of interest. The numerical values in the final column of the Table were computed for a minimum-mass solar nebula in “equilibrium” with $r_0 = 1\text{AU}$, $r_p = 10\text{cm}$, $\text{Re}_* = 180$, and $\text{Sc} = 3$. In these dimensionless units, equations (24)-(27) and (20) become *Table II goes here*

$$\frac{\partial(\Sigma_* V_*)}{\partial t_*} + \frac{\partial}{\partial x_*} \left(\Sigma_* U_* V_* - \nu_* \frac{\partial(\Sigma_* V_*)}{\partial x_*} \right) = -\frac{1}{2} \Sigma_* U_* - (1 + V_*) \frac{R_*}{2}, \quad (28)$$

$$\frac{\partial(\Sigma_* U_*)}{\partial t_*} + \frac{\partial}{\partial x_*} \left(\Sigma_* U_*^2 - \nu_* \frac{\partial(\Sigma_* U_*)}{\partial x_*} \right) = 2\Sigma_* V_* - U_* \frac{R_*}{2} - \Sigma_* \frac{\partial\psi_*}{\partial x_*} - \frac{\partial\Pi_*}{\partial x_*}, \quad (29)$$

$$\frac{\partial\Sigma_*}{\partial t_*} + \frac{\partial}{\partial x_*} \left(\Sigma_* U_* - \nu_* \frac{\partial\Sigma_*}{\partial x_*} \right) = 0, \quad (30)$$

$$\frac{\partial\Pi_*}{\partial t} + \frac{\partial}{\partial x_*} \left(U_* \Pi_* - \nu_* \frac{\partial\Pi_*}{\partial x_*} \right) = -2\Pi_* \frac{\partial U_*}{\partial x_*} - 2\gamma_*(\Pi_* - \Pi_{*0}), \quad (31)$$

$$\tilde{\psi}(k_*, t_*) = -\frac{2}{q_* |k_*|} e^{-|k_*| H_{*0}} \tilde{\Sigma}(k_*, t_*). \quad (32)$$

We have used the abbreviation

$$R_* \equiv \sqrt{U_*^2 + (1 + V_*)^2} \quad (33)$$

for the dimensionless form of the relative velocity (17).

2.5. Constant states

We will want to perform a linear stability analysis of eqs. (28)-(32) for small departures from a background situation in which the dependent variables are constant with respect to both x_* and t_* . We call this a “constant state.” When all of the derivative terms are set to zero, we have $\Pi_* \rightarrow \Pi_{*0}$, $\psi_* \rightarrow$ an irrelevant constant, and two algebraic relations,

$$\frac{1}{2} \Sigma_* U_* + (1 + V_*) \frac{R_*}{2} = 0 = 2\Sigma_* V_* - U_* \frac{R_*}{2}.$$

This leaves a one-parameter family of possible choices for (V_*, U_*, Σ_*) . Astrophysically, the choice is determined by the dust-to-gas ratio; at solar abundance, this is $\approx 1/200$, leading to $\Sigma_{*0} \approx 60$ at 1 AU as shown in Table II. While the global ratio is fixed by the initial conditions, the local one may vary, since even in the constant state, the dust drifts radially inward with respect to the gas. Depending upon the radial profile of gas density and temperature (which we have approximated by constants in our local approximation), this may lead to an enrichment or dilution of the dust at small radii.

So it is interesting to consider, at least briefly, the full range of possible constant states. The simplest equations result if one expresses Σ_* and U_* in terms of V_* . The physically allowed range is

$$-1 < V_* < 0, \quad (34)$$

and

$$\begin{aligned} U_* &= -\sqrt{-4V_*(1+V_*)}, \\ \Sigma_* &= (1+V_*)\sqrt{\frac{1-3V_*}{-4V_*}}. \end{aligned} \quad (35)$$

The dimensionless surface density is a monotonic function of V_* , but the radial velocity U_* is most negative at $V_* = -1/2$, where $-U_* = 1 = \Sigma_*$. (In physical units, this would imply an orbital decay time $r_0/|U|$ of only 160 yr at 1 AU!) In the limit $V_* \rightarrow -1$ and $\Sigma_* \rightarrow \infty$, drag is negligible because of the large inertia of the dust, which then follows exact keplerian orbits. In the opposite limit $V_* \rightarrow 0$ and $\Sigma_* \rightarrow 0$, the inertia of the dust is negligible and drag locks it to the gas. In both cases, the radial drift velocity vanishes. The simplicity of equations (35) motivated the choice of units shown in Table II, even though the nominal astrophysical values of the dimensionless variables are far from unity in this system.

A very important quantity is the radial mass flux,

$$F_* \equiv \Sigma_* U_* = -\sqrt{(1+V_*)^3(1-3V_*)} \approx -1 + O(V_*^2) \quad \text{if } |V_*| \ll 1, \quad (36)$$

so the mass flux is almost independent of the dust surface density in the astrophysically relevant parameter regime. Mass is the only globally conserved quantity in the dust layer—angular momentum is “lost” to the gas—and we may imagine that F_* is fixed by a boundary condition at large radius. The instabilities found below may be related to the fact that such a boundary condition constrains the constant state only very weakly.

3. LINEAR STABILITY

§3.1 analyzes a simplified problem in which both the self-gravity and the pressure of the dust layer are ignored. These simplifications allow the dispersion relation to be presented relatively easily in closed form. §3.2 presents numerical growth rates that incorporate both of these effects.

3.1. Analytic treatment without selfgravity or pressure

The simplified analysis is interesting for several reasons. First, it shows that self-gravity is not required for instability, the primary cause of which is the competition between drag and inertial forces. Second, the analysis provides a check on our numerically computed growth rates.

Finally, there are parameter regimes in which the neglected effects are unimportant—*e.g.*, pressure is inconsequential for large particles, which settle quickly to the midplane.

With Π_* and ψ_* neglected, only three of equations (28)-(32) are needed. We linearize the remaining three about an arbitrary constant state (35) and assume that the first-order quantities have the dependence

$$(\Delta U_*, \Delta V_*, \Delta \Sigma_*) \propto \exp [(z - \nu_* k_*^2) t_* + i k_* x_*]. \quad (37)$$

After considerable algebra (aided by commercial symbolic-manipulation software) we obtain a cubic dispersion relation for the shifted complex growth rate z :

$$\begin{aligned} 0 &= [(1 + 4w^2)(1 + w^2)^3] z^3 + [3w(w^2 + 1 - 2ik_*)(1 + 4w^2)(1 + w^2)^2] z^2 \\ &- [(48k_*^2 w^4 + 12k_*^2 w^2 - 8w^8 - 19w^6 - 15w^4 - 5w^2 - 1 + 56iw^6 k_* \\ &\quad + 70iw^4 k_* + 14iw^2 k_*)(1 + w^2)] z \\ &+ 8ik_* w^3 (-6w^4 + 8iw^4 k_* + 2ik_* + 4k_*^2 w^2 - 3w^2 + k_*^2 - 3w^6 + 10iw^2 k_*). \end{aligned} \quad (38)$$

To avoid radicals in the coefficients, we have introduced an auxiliary variable w defined by

$$V_* = -\frac{w^2}{1 + w^2}, \quad 0 < w < \infty. \quad (39)$$

Nevertheless, the dispersion relation is cumbersome and best understood in limiting cases.

First, as $w \rightarrow \infty$, *i.e.* the state $(U_*, V_*, \Sigma_*) \rightarrow (0, -1, 0)$ where the dust layer is pinned to the gas, there are two rapidly damped roots $z \approx -w$ and $z \approx -2w$. The interesting root is the third one:

$$z \approx 3ik_* w^{-1} + \frac{1}{2} k_*^2 w^{-3}, \quad (w \rightarrow \infty), \quad (40)$$

where we show only the leading order terms in the real and imaginary parts. The actual growth rate, however, is $\text{Real}(z) - \nu_* k_*^2$. Therefore, since $\Sigma_* \approx w^{-2}$ in this limit, the system is stable if $\Sigma_* < (2\nu_*)^{2/3}$.

The more important limit is $w \rightarrow 0$, $(U_*, V_*, \Sigma_*) \rightarrow (0, 0, \infty)$. If one assumes that k_* and z are of order unity and sets $w = 0$ above, then the dispersion relation (38) reduces to $z^3 + z = 0$. This has two purely imaginary roots $z = \pm i$, corresponding to modes that will damp for any $\nu_* > 0$. To study the root near $z \approx 0$, one has to go to higher order:

$$z \approx (2k_*^2 - ik_*^3) \Sigma_*^{-3} \quad [w \rightarrow 0, \Sigma_* \rightarrow \infty, k_* \sim O(1)]. \quad (41)$$

This indicates instability if $\Sigma_* < (2/\nu_*)^{1/3}$. In extracting the approximate root (41) from eq. (38), we assumed that k_* is of order unity. But if we take $k_* = q/w$ with $q \sim O(1)$ as $w \rightarrow 0$, a different ordering of terms results, and the dispersion relation reduces approximately to

$$(\omega')^3 - (\omega') + 2q = 0, \quad \omega' \equiv iz + 2q. \quad (42)$$

Clearly, if $|q|$ is sufficiently large, then there are a pair of complex-conjugate roots for ω' , implying the existence of a root for z with positive real part. The corresponding growth rate is approximately

$$3^{1/2}2^{-2/3}q^{1/3} - \nu_*(q/w)^2.$$

The maximum growth rate is therefore

$$\text{Real}(z)_{\max} \approx 0.49\Sigma_*^{-2/5}\nu_*^{-1/5} \quad (\Sigma_* \rightarrow \infty). \quad (43)$$

which is achieved at $q \approx 0.31(\Sigma_*^2\nu_*)^{-3/5}$. But (42) has complex roots only if $|q| > 3^{-3/2}$, and so this growing mode exists only if $\Sigma_* < 1.5\nu_*^{-1/2}$, approximately.

Scrutiny of Table II shows that the combination $\Sigma_*^2\nu_*$ is independent of the critical Reynolds number Re_* . Therefore, the maximum growth rate is formally independent of this most uncertain parameter. The same is true for the ratio $2\pi(k_*H_{*0})^{-1}$ of wavelength to dust-layer thickness at maximum growth.

To summarize, if $0 < \nu_* \ll 1$, then constant states are unstable when $\nu_*^{2/3} \lesssim \Sigma_* \lesssim \nu_*^{-1/2}$. Selfgravity will probably enlarge the range of instability, while pressure will probably reduce it, but both effects introduce additional uncertain parameters.

3.2. Numerical Growth Rates

As a complement to the analytic treatment of the previous section, we performed a numerical linear stability analysis of the governing equations so as to investigate the effects of pressure and self-gravity upon the expected growth rates. We began our analysis by transforming the governing equations into Fourier space. In this way, the gravitational potential can be eliminated in favor of the surface density via Poisson's eq. (20). We next recast the equations by introducing new variables for the radial and azimuthal mass flux; $f \equiv \Sigma_*U_*$: $j \equiv \Sigma_*V_*$. We then proceeded to linearize the governing equations about the constant states by adding a perturbation to each dynamic variable (ie. $f \rightarrow f + \Delta f$), expanding, and then only retaining those terms which are linear in the perturbations. Thereby, with $\hat{z} \equiv \partial/\partial t_* - \nu_*\partial^2/\partial x_*^2$, we wrote the system of linearized governing equations in the form

$$\hat{z}(\mathbf{y}) = \mathcal{L}\mathbf{y},$$

where $\mathbf{y} = (\Delta f, \Delta j, \Delta\Sigma_*, \Delta\Pi_*)$ is the vector of first-order dynamic variables. Then, given the form of the (x_*, t_*) dependence (37), it follows that the eigenvalues of the linear operator matrix, $\lambda_{\mathcal{L}}$, correspond to dimensionless growth rates = $\text{Re}(\lambda_{\mathcal{L}}) - \nu_*k_*^2$.

This analysis was performed for a range of plausible nebula parameters, specifically; r (orbital radius) $\in \{0.1 \text{ AU}, 1.0 \text{ AU}, 10 \text{ AU}\}$, r_p (particle size) $\in \{0 \text{ cm}, 10 \text{ cm}, 100 \text{ cm}\}$, $\text{Re}_* \in \{45, 70, 180, 500\}$. Figure 1 shows the growth rate as a function of wavenumber for various parameter values. For reference, the unperturbed surface density in our model is about an order

of magnitude lower than the critical surface density required for the Goldreich-Ward dynamical instability.

Fig. 1

For most choices of the background parameters, the growth rate is largest at the shortest available wavelengths. We present results down to a wavelength comparable to the dust layer thickness, as the validity of the height-integrated approach is questionable beyond this point. There are a few sets of nebula parameters, however, for which the peak growth rate occurs on a significantly larger spatial scale. Fig. 2 shows the growth rates for nebula parameters $r = 0.1$ AU, $r_p = 10$ cm, $\text{Re}_* = 180$. Again, rates are shown with and without self-gravity. These growth rates are notably different from those at other parameter values in that they are considerably lower and become negative for all wavenumbers in the absence of self-gravity.

It is our interpretation that there are two distinct secular instabilities in this system. One is the self-gravitating secular instability discussed in §1. It has a relatively low growth rate and a long radial wavelength compared to the dust-layer thickness. This is the instability which appears in Fig. 2. The other is the drag-induced instability discussed in the previous section, which has larger growth rates and shorter wavelengths, and is exhibited in Fig. 1. Probably because of its large growth rate, the drag instability is found over a wider range of relevant nebular and particle parameters. The rest of the results in this section refer to instances in which the drag instability dominates.

Fig. 2

Table III. presents the peak growth rate achieved for a number of other prominent sets of nebula parameters. Generally, the dimensionless growth rates

Table III here

i) increase monotonically with increasing orbital radius. An increase in orbital radius implies a decrease in the surface dust density and an increase in the dust scale height. [The orbital radius also effects the stopping time by determining the drag regime.]

ii) increase with increasing particle size. An increase in particle size implies an increase in the settling rate.

iii) increase with increasing critical Reynolds number. An increase in Reynolds number implies an increase in the dust surface density and a decrease in the dust scale height.

We repeated the above analysis with the terms relevant to pressure and self-gravity selectively neglected.¹ As expected, the growth rates are larger without pressure and smaller without self-gravity. But the changes are typically on the order of ten to twenty percent. When both pressure and self-gravity are neglected, we recover the growth rates predicted by the cubic dispersion relation (38).

In summary, our linear analysis reveals a drag-induced instability which grows most rapidly

¹Recall that in this context, “pressure” means the excess height-integrated pressure due to the weight of the local dust column, cf. §2.3.

on short wavelengths at large orbital radii, for large particles, and high critical Reynolds number.

4. DISCUSSION

We have shown that for plausible nebular parameters, the growth rate of the drag instability can be comparable to the orbital frequency Ω .

The instability is rather robust. The following toy model shows that the *tendency* to instability—as opposed to the actual growth rate—does not depend upon the more intricate and uncertain assumptions that we have made in formulating our dynamical equations. Consider a one-dimensional distribution of mass $\sigma(x, t)$ per unit length that is subject to a fixed “gravitational” acceleration g and an opposing “frictional” force per unit length $-f(\sigma)v$. Here σg is a proxy for the gravitational and coriolis terms in the dust-layer equation of motion—forces that are proportional to mass—whereas f stands for the drag force on the surface of the dust layer, which is essentially independent of the surface mass density. The equations for mass and velocity (v) are

$$\begin{aligned}\partial_t \sigma + \partial_x(\sigma v) &= 0, \\ \partial_t v + v \partial_x v &= g - v f(\sigma)/\sigma,\end{aligned}$$

This system has equilibria with uniform velocity v_0 and surface density σ_0 satisfying $\sigma_0 g = f(\sigma_0)$. Without loss of generality, $v_0 = 0$. Linear perturbations with (x, t) dependence $\exp(st + ikx)$ have the dispersion relation

$$s^2 = -ik \frac{d}{d \ln \sigma} \left(\frac{f}{\sigma} \right) \Big|_{\sigma=\sigma_0}$$

Clearly, there will always be an unstable root, $\text{Real}(s) > 0$, regardless of the details of the friction function $f(\sigma)$, unless the frictional force is strictly proportional to mass. One could certainly complicate to this model to stabilize it, but the point is that a balance between inertial and non-inertial forces tends to be unstable.

The one assumption that is truly critical for instability is that drag should act coherently upon the dust layer as whole. If the drag acts upon each particle independently, collective instability cannot result from drag alone. The assumption of collective drag, introduced by GW, is reasonable if the gas within the dust layer is substantially entrained by the dust, which requires that the turbulent wakes of particles overlap before they mix with the gas above and below the dust layer. The net drag will then be less than it would be if each particle independently encountered the full headwind from the subkeplerian gas. Thus, a necessary condition for the drag to be treated as a collective effect is that the force per unit area (3) be less than $N \times f(r_p)$, where $f(r_p)$ is the drag on an isolated (spherical) particle of radius r_p , and N is the number of such particles per unit area. For simplicity, let the dust layer be composed entirely of particles having this radius; then the surface density of the layer is related to r_p by

$$\frac{4\pi}{3} \rho_s r_p^3 N = \Sigma_p, \tag{44}$$

where $\rho_s \approx 1 \text{ g cm}^{-3}$ is the density of the solid material. In the size regime $r_p \sim 10 - 100 \text{ cm}$, the drag on this particle can be estimated from Stokes formula,

$$f(r_p) = 6\pi\mu_g r_p \Delta v, \quad (45)$$

with dynamical viscosity $\mu_g \approx 0.9 \times 10^{-4} \text{ g/cm-s}$ at 300 K. Thus

$$\frac{F_{\text{drag}}^{\text{collective}}}{Nf} \approx \frac{2r_p^2 \rho_s \rho_g \Delta V}{9\text{Re}_* \Sigma_p \mu_g} \approx 0.08 \left(\frac{\text{Re}_*}{180} \right)^{-1} \left(\frac{a}{1 \text{ AU}} \right)^{-1} \left(\frac{r_p}{100 \text{ cm}} \right)^2, \quad (46)$$

using the nebular parameters and scalings of equations (2) and Table I, and assuming that $\Delta V \approx c^2/V_K$. Actually, the force ratio (46) is independent of the temperature and density profile of nebula as long as the relative abundance Σ_g/Σ_p of gas and dust is constant. We conclude from this that a collective treatment of the drag is appropriate as long as $r_p \lesssim 3 \text{ m}$.

Several groups have previously analyzed the stability of disks when gas and dust are treated as dynamically distinct components, but none of them seem to have identified the drag instability that we have emphasized, and it is interesting to ask why not. Coradini et al. (1981) performed a stability analysis local to the interior of the dust layer, where the dust was treated as uniformly mixed into the gas but enhanced in abundance by sedimentation. Their vertically local treatment overlooked the exchange of angular momentum between the layer as a whole and the relatively dust-free overlying gas. The approach of Sekiya & Nakagawa (1988) was similar, except that they allowed for more general perturbed velocities within the layer (not necessarily parallel to the midplane). Both of these groups found instabilities, but only for dust densities larger than the critical value ρ_* (cf §1), so these presumably were modes that rely upon selfgravity. Noh et al. (1991) investigated global *nonaxisymmetric* stability of the disk. They allowed for a thin dust layer but represented the drag force by a term strictly proportional to mass, which suppresses the nonselfgravitating drag instability, as the toy model above demonstrates. Noh et al. (1991)'s approximations should have captured the secular selfgravitating mode sketched in §1 if they had considered axisymmetric modes; they may have found a nonaxisymmetric version of the instability but did not interpret their results along these lines [see their Fig. (4b)].

Is the drag instability necessary to form planetesimals, or will collisional agglomeration may accomplish the task more quickly? There are at least two issues:

- (i) Do collisions result in larger particles, *i.e.*, do colliding particles stick or fragment?
- (ii) How does the collision rate compare with the growth rate of the drag instability?

The first question is difficult because one does not understand the structure and elastic strength of the particles. If these are loose aggregates, fragmentation is likely at relative velocities $> 10 \text{ m s}^{-1}$ (Weidenschilling & Cuzzi 1993, and references therein).

As for the second question, it is clear that the collision rate is as fast or probably faster than the drag instabilities. If all particles are spheres of radius r_p , then the probability of crossing the

dust layer without a collision is $\sim \exp(-3\Sigma_p/\rho_p r_p)$, so that the collision rate per particle

$$(\Omega t_{\text{coll}})^{-1} \sim \frac{\Sigma_p}{2\rho_p r_p} \approx 0.13 \left(\frac{r_p}{1 \text{ m}}\right)^{-1} \left(\frac{a}{\text{AU}}\right)^{-3/2} \text{ yr}^{-1} \quad (47)$$

for the nebular parameters of Table I.

Therefore, if most collisions result in sticking, then collisional agglomeration is probably more important than drag instability. But, it is interesting that the latter process is at competitive with collisions. The collective instability has the attractive feature that it may take planetesimals directly from sizes $\sim 10 \text{ cm}$ to $\sim 1 \text{ km}$ in a single step, and thereby bypass the size regime in which orbital decay (due to aerodynamic drag on individual planetesimals) is dangerously rapid.

Assuming that the collective instability does operate, it will be important to understand the nonlinear outcome. We have performed time-dependent numerical integrations of the nonlinear system (28)-(31), neglecting selfgravity and pressure. Typically, the surface density peaks an order of magnitude or more above the background. No simple pattern emerges; multiple peaks develop at slightly different radial drift speeds. Numerical stability does not seem to be an issue as long as a suitably short time step is used, but unfortunately, the detailed nonlinear outcome depends upon the form chosen for the diffusive terms. In eqs. (28)-(31), the diffusive terms are in “flux-conservation” form, but there is no clear reason to demand such a form except in the mass equation (31), since radial and azimuthal momentum can be exchanged with the gas. We found nonconservative forms that produced the same linear growth rates but more organized nonlinear evolution. Because of these uncertainties, and because selfgravity and nonaxisymmetry would have to be included in order to understand planetesimal formation, we shall not give details of our nonlinear experiments.

Nevertheless, we cannot resist using the linear results to speculate about the mass of the planetesimals that may form by this instability. Since the linear growth rate appears to peak at a wavelength of order $4\pi H_p$ (Fig. 1), a plausible estimate for the mass is

$$M_{\text{planetesimal}} \sim \Sigma_p (2\pi H_p)^2 \sim 3 \times 10^{19} \text{ g}. \quad (48)$$

The numerical value is evaluated for the surface density and thickness of the dust layer at 1 AU (Table I). After expulsion of gas and collapse to solid densities, this corresponds to a planetesimal radius $\sim 10 \text{ km}$ —larger than for GW’s direct gravitational instability because our dust layer is thicker than theirs.

5. SUMMARY

We have found a new collective instability of the dust layer in a quiescent protostellar disk. Like the gravitational instability contemplated by Safronov (1969) and Goldreich & Ward (1973), the new one may collect particles smaller than a meter directly into planetesimals larger than a kilometer, thereby circumventing a possible difficulty with rapid orbital decay of the particles. But

the new instability is driven by drag rather than selfgravity. In fact, it is driven by the very shear turbulence that limits the density of the dust layer and forestalls direct gravitational instability. We envision a two-stage mechanism in which drag first concentrates the dust radially into rings until they become selfgravitating, whereupon the rings fragment nonaxisymmetrically. We find that instability is generic when inertial forces balance frictional forces in a nonrigid mass layer. Thus, the tendency to instability is independent of the details of the dynamical equations we have used to describe the dust layer. To the extent that these equations are correct and that the parameters of a standard minimum-mass solar nebula are applicable, the growth time of the drag instability is of order the orbital period and comparable to the two-body collision time. Planetesimals formed by this instability are estimated to have radii of order 10 km at 1 AU.

These conclusions are subject to several caveats. Most importantly, we lack a fundamental understanding of the exchanges of momentum and mass between the dust and gas layers. Turbulence is central to these exchanges, and we are unaware of any directly comparable terrestrial analogs to the dust layer, which is probably better described as a slurry than the flat plate envisaged by Goldreich and Ward. Formally at least, our growth rates are rather insensitive to the critical Reynolds number Re_* , which describes both the drag on the dust layer and its thickness (§2 & §4), and to the particle size. Most likely, however, these parameters must lie within a limited range if our dynamical equations are to be valid. It is vital for the drag instability that the drag on the dust layer be treated as a collective process. According to our best estimates, a collective model is appropriate for particles smaller than about 3 meters at 1 AU, and this limiting size depends upon Re_* (§4). On the other hand, when the particles are much smaller than 10 cm, shear-driven turbulence may not be fully developed, so that the drag and the growth rate may be substantially reduced (§2.2). Also, the equilibration time of the dust-layer thickness is a strong function of particle size; there may be parameter regimes in which drag quickly produces large contrasts in surface density, but gravitational instability has to wait for particles to settle and the volume density to increase. Direct numerical simulations of dust-gas mixtures in three dimensions may be necessary to answer these questions.

This work was supported by the NASA Origins program under grant NAG5-8385.

REFERENCES

- Balbus, S. A. & Hawley, J. F. 1998. Instability, Turbulence, and Enhanced Transport in Accretion Disks. *Rev. Mod. Phys.* **70**, 1-53.
- Beckwith, S. V. W., Henning, T., & Nakagawa, Y. 1999. Dust Properties and Assembly of Large Particles in Protoplanetary Disks. In *Protostars and Planets IV* (V. Manning & A. Boss, eds.), University of Arizona Press, Tucson (in press); also astro-ph/9902241.
- Chandrasekhar, S. 1987. *Ellipsoidal Figures of Equilibrium*, Dover, New York.

- Coradini, A., Federico, C., & Magni, G. 1981. Formation of Planetesimals in an Evolving Protoplanetary Disk. *Astron. Astrophys.* **98**, 173-185.
- Cuzzi, J. N., Dobrovolskis, A. R., & Champney, J. M. 1993. Particle-gas dynamics in the midplane of a protoplanetary nebula. *Icarus* **106**, 102-134 (CDC).
- Drazin, P. G. & Reid, W. H. 1981. *Hydrodynamic stability*, Cambridge University Press, Cambridge.
- Goldreich, P. & Ward, W. R. 1973. The Formation of Planetesimals. *Astrophys. J.* **183**, 1051-1061 (GW).
- Hayashi, C., Nakazawa, K., & Nakagawa, Y. 1985. In *Protostars and Planets II*, (D. C. Black & M. S. Matthews, eds.), University of Arizona Press, Tucson, pp. 1100-1153. Formation of the Solar System.
- Noh, H., Vishniac, E. T., & Cochran, W. D. 1991. Gravitational Instabilities in a Proto-planetary Disk. *Astrophys. J.* **383**, 372-379.
- Pedlosky, J. 1987. *Geophysical Fluid Dynamics*, Second Edition Springer-Verlag, New York.
- Safronov, V. S. 1969, *Evolution of the Protoplanetary Cloud and Formation of the Earth and the Planets*, Nauka, Moscow. Transl. Israel Program for Scientific Translations, v. 206, NASA Technical Translations NASA-TT F-677 (1972).
- Safronov, V. S. 1991. Kuiper prize lecture: Some problems in the formation of the planets. *Icarus* **94**, 260-271.
- Schmit, U. & Tscharnuter, W. M. 1995. A Fluid Dynamical Treatment of the Common Action of Self-Gravitation, Collisions, and Rotation in Saturn's B-Ring *Icarus* **115**, 304-319.
- Sekiya, M. 1998. Quasi-Equilibrium Density Distributions of Small Dust Aggregations in the Solar Nebula. *Icarus* **133**, 298-309.
- Sekiya, M. & Nakagawa, Y. 1988. Settling of Dust Particles and Formation of Planetesimals. *Prog. Theor. Phys. Suppl.* **96**, 141-150.
- Weidenschilling, S. J. 1977. Aerodynamics of solid bodies in the solar nebula. *Mon. Not. R. Astron. Soc.* **180**, 57-70.
- Weidenschilling, S. J. 1980. Dust to Planetesimals: Settling and Coagulation in the Solar Nebula. *Icarus* **44**, 172-189.
- Weidenschilling, S. J., & Cuzzi, J. N. 1993. Formation of Planetesimals in the Solar Nebula. In *Protostars and Planets III* (E. H. Levy & J. I. Lunine, eds.), University of Arizona Press, Tucson, pp. 1031-1060.

TABLE I

Physical parameters of the protoplanetary disk and dust layer: symbols, meanings, and assumed numerical values.

Symbol	Meaning	Formula	Nominal Value (1AU)
c	isothermal sound speed	$\sqrt{k_B T / \bar{\mu}}$	1.0 km s ⁻¹
c_L, c_δ	boundary-layer factors	—	1.5, 2.5
η	azimuthal drift factor	$(V_K - V_{\text{gas}})/V_K$	10 ⁻³
H_g	gas-layer $\frac{1}{2}$ -thickness	c/Ω	5.1×10^6 km
H_p	dust-layer $\frac{1}{2}$ -thickness	$c_L c_\delta \eta r_0 / \text{Re}^*$	3.1×10^3 km
V_K	keplerian velocity	$\sqrt{GM/r_0}$	30 km s ⁻¹
Ω	orbital angular velocity	V_K/r_0	2π yr ⁻¹
r	orbital radius	—	1 AU
Re^*	critical Reynolds number	—	180
Sc	Schmidt number	—	1.0
Σ_g	gas surface density	—	1700 g cm ⁻²
Z_p	dust abundance by mass	—	0.005
Σ_p	dust surface density	$Z_p \Sigma_g$	8.5 g cm ⁻²
U_0	radial drift speed	$-2\rho_g(\eta V_K)^2 / \text{Re}_* \Omega \Sigma_p$	-1.0 m s ⁻¹

TABLE II

Dimensionless variables and parameters.

Symbol	Meaning	Definition	Nominal Value
<i>Dimensional Units</i>			
T_1	time	Ω^{-1}	1 yr/ 2π
L_1	length	ηr_0	10^{-3} AU
S_1	surface density	$2\rho_g \eta r_0 / \text{Re}_*$	0.28 g cm $^{-2}$
<i>Independent variables</i>			
t_*	time	$t \cdot \Omega$	—
x_*	radial separation	$(r - r_0) / L_1$	—
k_*	radial wavenumber	$k \cdot L_1$	—
<i>Dependent variables</i>			
Σ_*	surface density	Σ_p / S_1	30.
U_*	radial drift speed	$U / \eta V_K$	–0.033
V_*	azimuthal drift	$V / \eta V_K$	-2.8×10^{-4}
Π_*	2D pressure	$\Pi / S_1 (\eta V_K)^2$	0.013
ψ_*	self-potential	$\psi / (\eta V_K)^2$	—
<i>Dimensionless constant parameters</i>			
ν_*	diffusivity	$c_L^2 / \text{Re}_*^2 \text{Sc}$	2.3×10^{-5}
H_{*0}	equil. $\frac{1}{2}$ -thickness	$c_\delta c_L / \text{Re}_*$	0.021
Π_{*0}	equil. pressure	$\Sigma_{*0} H_{*0}^2$	0.013
q_*	self-gravity	$\eta V_K \Omega / \pi G S_1$	1.0×10^4
γ_*	settling rate	Ωt_s	0.11

TABLE III

Local axisymmetric instabilities of the dust layer. Numerical growth rates (column 4) are given in units of local orbital frequency Ω .

r_p (cm)	r (AU)	Re_*	Maximum growth rate	e -folding time (yr)	Comments
0	0.1	180	1.8×10^{-4}	28.0	
10	0.1	45	2.1×10^{-4}	24.0	long-wavelength instability
10	0.1	180	1.9×10^{-4}	26.5	
10	0.1	500	0.30	1.7×10^{-2}	
100	0.1	180	0.24	2.1×10^{-2}	
0	1.0	180	0.46	0.35	
10	1.0	45	0.45	0.35	nominal parameters
10	1.0	180	0.55	0.29	
10	1.0	500	0.69	0.23	
100	1.0	180	0.73	0.22	
0	10.0	180	0.78	6.45	
10	10.0	180	0.76	6.49	
10	10.0	180	0.90	5.58	
10	10.0	180	1.01	4.96	
100	10.0	180	0.94	5.31	

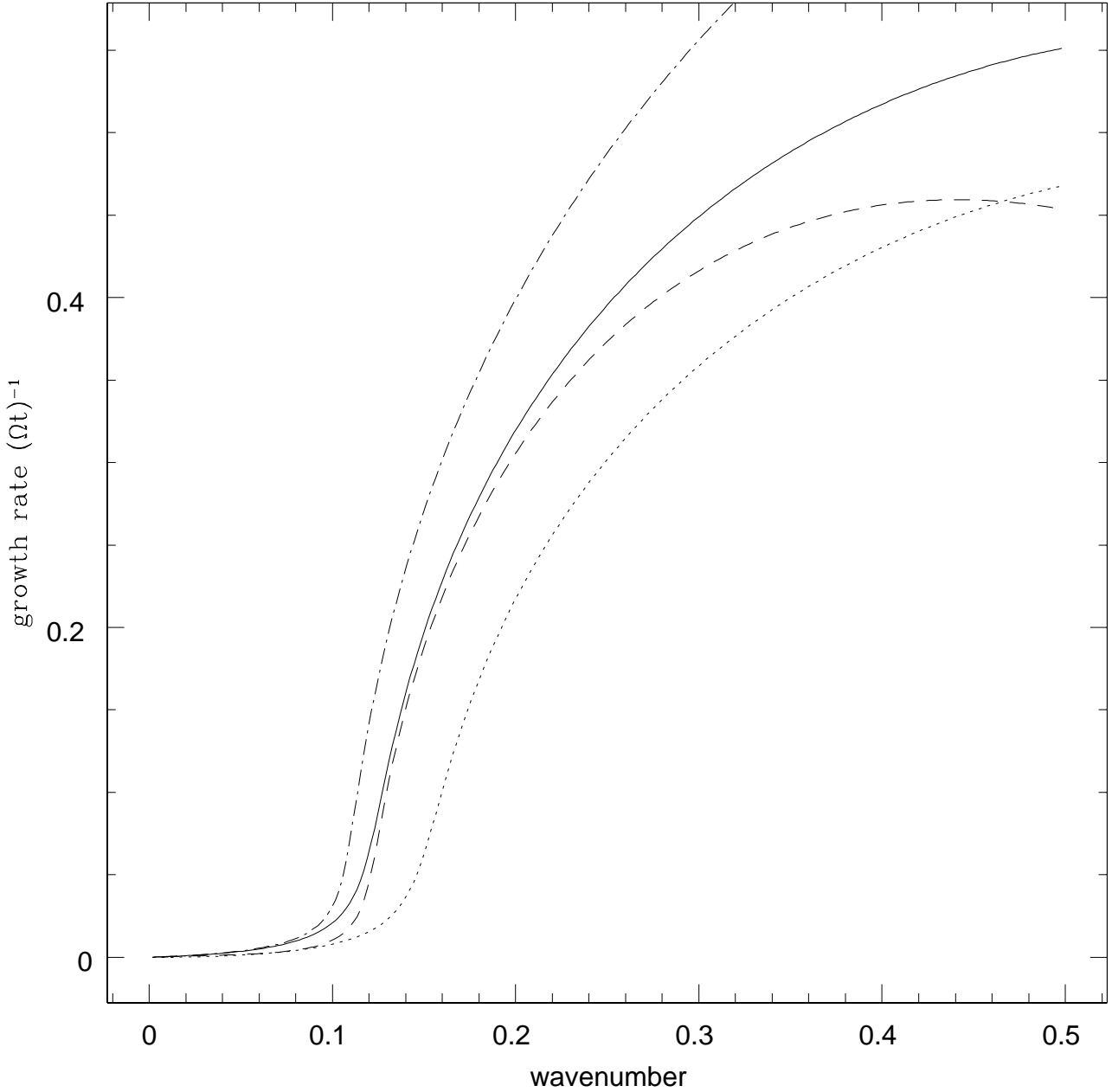


FIG. 1. Dimensionless linear growth rates for nebula parameters $r = 1$ AU, $\text{Re}_* = 180$. The four curves represent models for $r_p = 10$ cm with (solid line) and without (short dashed) self-gravity, as well as for $r_p = 0$ cm (dashed) and $r_p = 100$ cm (dot-dashed), both with self-gravity. The units of wavenumber are such that a wavenumber of 1.0 corresponds to an instability at a wavelength of $2\pi H_p$.

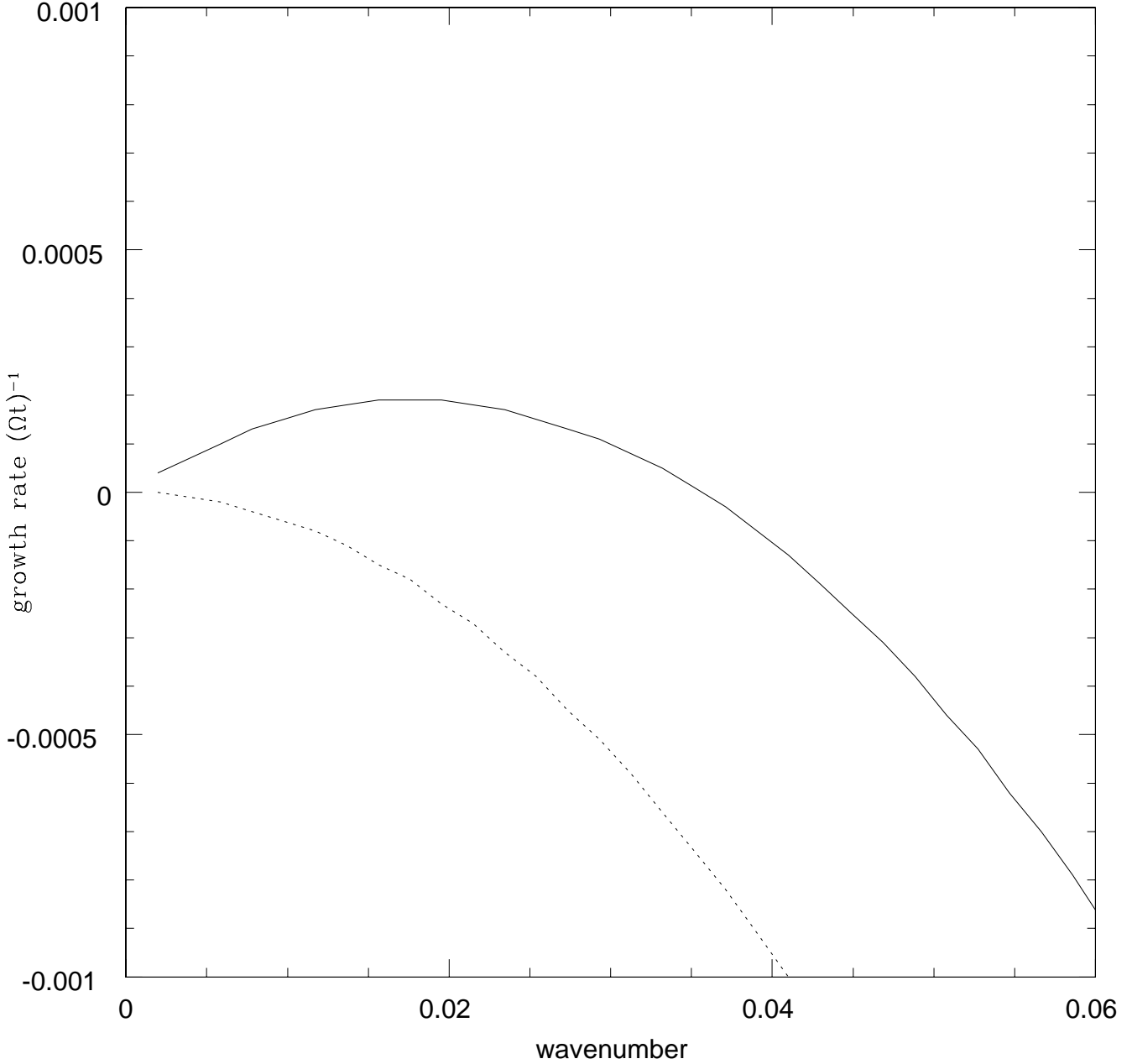


FIG. 2. Dimensionless linear growth rates for nebula parameters $r = 0.1$ AU, $r_p = 10$ cm, $\text{Re}_* = 180$. The two curves represent models with (solid line) and without (short dashed) self-gravity. The instability for this set of nebula parameters is slowly-growing, occurs at long wavelengths, and is not seen in the absence of self-gravity. The units of wavenumber are such that a wavenumber of 1.0 corresponds to an instability at a wavelength of $2\pi H_{*0}$.